Circulation

ORIGINAL RESEARCH ARTICLE

A Unique Population of Regulatory T Cells in Heart Potentiates Cardiac Protection From Myocardial Infarction

Ni Xia, MD, PhD*
Yuzhi Lu, MD, PhD*
Muyang Gu, MD, PhD*
Nana Li, MD, PhD
Meilin Liu, MD
Jiao Jiao, MD, PhD
Zhengfeng Zhu, MD, PhD
Jingyong Li, MD, PhD
Dan Li, MD, PhD
Tingting Tang, MD, PhD
Bingjie Lv, MD, PhD
Shaofang Nie, MD, PhD
Min Zhang, MD, PhD
Mengyang Liao, MD, PhD
Yuhua Liao, MD, PhD
Xiangping Yang, PhD
Xiang Cheng, MD, PhD

BACKGROUND: Regulatory T cells (Tregs), traditionally recognized as potent suppressors of immune response, are increasingly attracting attention because of a second major function: residing in parenchymal tissues and maintaining local homeostasis. However, the existence, unique phenotype, and function of so-called tissue Tregs in the heart remain unclear.

METHODS: In mouse models of myocardial infarction (MI), myocardial ischemia/reperfusion injury, or cardiac cryoinjury, the dynamic accumulation of Tregs in the injured myocardium was monitored. The bulk RNA sequencing was performed to analyze the transcriptomic characteristics of Tregs from the injured myocardium after MI or ischemia/reperfusion injury. Photoconversion, parabiosis, single-cell T-cell receptor sequencing, and adoptive transfer were applied to determine the source of heart Tregs. The involvement of the interleukin-33/suppression of tumorigenicity 2 axis and Sparc (secreted acidic cysteine-rich glycoprotein), a molecule upregulated in heart Tregs, was further evaluated in functional assays.

RESULTS: We showed that Tregs were highly enriched in the myocardium of MI, ischemia/reperfusion injury, and cryoinjury mice. Transcriptomic data revealed that Tregs isolated from the injured hearts had plenty of differentially expressed transcripts in comparison with their lymphoid counterparts, including heart-draining lymphoid nodes, with a phenotype of promoting infarct repair, indicating a unique characteristic. The heart Tregs were accumulated mainly because of recruitment from the circulating Treg pool, whereas local proliferation also contributed to their expansion. Moreover, a remarkable case of repeatedly detected T-cell receptor of heart Tregs, more than that of spleen Tregs, suggests a model of clonal expansion. Besides, Helios^{high}Nrp-1^{high} phenotype proved the mainly thymic origin of heart Tregs, with a small contribution of phenotypic conversion of conventional CD4$^+$ T cells, proved by the analysis of T-cell receptor repertoires and conventional CD4$^+$ T cells adoptive transfer experiments. The interleukin-33/suppression of tumorigenicity 2 axis was essential for sustaining heart Treg populations. Last, we demonstrated that Sparc, which was highly expressed by heart Tregs, acted as a critical factor to protect the heart against MI by increasing collagen content and boosting maturation in the infarct zone.

CONCLUSIONS: We identified and characterized a phenotypically and functionally unique population of heart Tregs that may lay the foundation to harness Tregs for cardioprotection in MI and other cardiac diseases.

*Drs Xia, Lu, and Gu contributed equally.

Key Words: collagen ■ heart rupture ■ myocardial infarction ■ osteonectin ■ T-lymphocytes, regulatory

Sources of Funding, see page 1972

https://www.ahajournals.org/journal/circ

Clinical Perspective

What Is New?

- We demonstrate that regulatory T cells (Tregs) that accumulate in the injured myocardium after myocardial infarction (MI) or myocardial ischemia/reperfusion injury have a distinct transcriptome, which differs from lymphoid organ Tregs and other nonlymphoid tissue Tregs, representing a novel population of tissue Tregs.
- Heart Tregs, which are mainly thymus-derived Tregs recruited from circulation, show active local proliferation, with the interleukin-33/suppression of tumorigenicity 2 axis promoting their expansion.
- With the phenotype of promoting tissue repair, heart Tregs overexpressing Sparc (secreted acidic cysteine-rich glycoprotein) contribute to elevated collagen content and enhanced maturation in infarct scars to prevent cardiac rupture and improve survival after MI.

What Are the Clinical Implications?

- This study revealed a special population of tissue Tregs with a unique phenotype and prorepair function in the MI-injured hearts, providing a novel target for the clinical treatment of MI.
- These findings may stimulate further study of Tregs as a cell-based therapy, such as induction of heart Tregs in MI and other cardiac diseases.

Regulatory T cells (Tregs), especially the subset of $CD4^+Foxp3^+$ Tregs, are critical in maintaining immune homeostasis and regulating inflammatory disease progressions.[1] Tregs can modulate the activation and function of a variety of immunocytes, including innate and adaptive immune system players.[2] In addition to their immunoregulatory function, existing evidence shows that Tregs have extraimmunologic roles, for example, promoting effective tissue repair in peripheral tissues.[3] The initial research on tissue-resident Tregs came from the Mathis team that described the characteristics of visceral adipose tissue Tregs and injured muscle Tregs.[4–6] Visceral adipose tissue Tregs highly express peroxisome proliferator–activated receptor-gamma and enhance glucose metabolism in adipocytes, which mitigates insulin resistance.[4,5] However, injured muscle Tregs express Areg (amphiregulin), targeting the muscle satellite cells and maintaining tissue integrity.[6] Since then, Tregs with unique phenotypes and functions have been reported in the pancreas,[7] skin,[8] brain,[9] and lung.[10] Tregs in the hearts, especially undergoing myocardial infarction (MI), however, remain largely undefined.

MI is one of the most common cardiovascular diseases, with ventricular rupture and heart failure as its major causes of death. Therefore, preventing cardiac rupture and controlling ventricular remodeling in the early and late stages, respectively, can effectively improve clinical outcomes.[11] A variety of immune components, including Tregs, are involved in the repair after MI.[12–14] Elimination and expansion experiments confirmed that Tregs play a protective role in MI by alleviating local inflammation, protecting cardiomyocytes from apoptosis, and modulating macrophage differentiation and myofibroblast activation.[12–14] However, these findings leave open the question: What is the characteristic of Tregs themselves in MI hearts? Specifically, whether Tregs have local adaption with unique phenotype, how the populations accumulate in MI hearts and what factors drive their accumulation are largely unknown. It is most important to note that whether they were endowed with unique functions in hearts such as directly targeting the cardiac repair process independent of immune regulation remains to be fully elucidated.

In the present study, we set up to investigate the characteristic of Tregs accumulated in MI hearts through multiple transcriptional and functional assays. The results revealed a unique population of tissue-related Tregs in the hearts after MI, characterized their distinct phenotypes, sources, and sustaining factors, and support the emerging role of Tregs in cardiac repair. Our study therefore provided insight into developing new therapy for the clinical treatment of MI by using Tregs.

METHODS

On reasonable request, the data that support the findings of this study are available from the corresponding author. Extended methods are provided in the Data Supplement.

Animals

All mice used in our study were housed under specific pathogen-free conditions. All animal studies were conducted according to the criteria outlined in the "Guide for the Care and Use of Laboratory Animals" prepared by the National Academy of Sciences and published by the National Institutes of Health (NIH publication 86-23 revised 1985) and approved by the Animal Care and Utilization Committee of Huazhong University of Science and Technology, China. The procedures followed were in accordance with institutional guidelines.

Reverse Transcription Polymerase Chain Reaction

Total RNA was extracted using TRIzol reagent, and mRNA levels were quantified by reverse transcription polymerase chain reaction (RT-PCR). The primers used for RT-PCR are listed in Table I in the Data Supplement.

Statistical Analysis

Data are presented as the mean±SEM. The Kolmogorov-Smirnov test with Lilliefors correction was first used to

determine data normality, and the F test was used to determine equal variance. If the data passed the evaluation of normality and similar variances, statistical significance was determined by 1- or 2-way ANOVA with Tukey post hoc multiple comparisons tests to analyze differences among ≥3 groups, or by unpaired Student *t* test to analyze the differences between 2 groups. The nonparametric tests, such as Kruskal-Wallis test, Scheirer-Ray-Hare test, or Mann-Whitney *U* test were used when the data displayed abnormal distribution, and these data were presented in the form of box-and-whisker plots to show the median and ranges. Survival curves were obtained by the Kaplan-Meier method and compared by the log-rank test. In all cases, a 2-tailed *P* value of <0.05 was considered statistically significant. Statistical analysis was performed using GraphPad Prism 8.0.

RESULTS

Tregs Are Accumulated in the Injured Myocardium

To monitor the infiltration of heart Tregs at various times after MI, the dynamic analysis was performed by flow cytometry. The gating strategy of Tregs in hearts is shown in Figure 1A. Tregs in the sham-operated hearts, spleens, or peripheral blood were evaluated separately. Tregs in myocardium had a tendency to increase at day 1 post-MI, reached the highest value at day 7, and still maintained increased values at day 14 (Figure IA in the Data Supplement). The number of heart CD4$^+$ T cells and heart conventional T cells (Tconvs) both peaked at day 7 after MI, parallel to heart Tregs (Figure IB and IC in the Data Supplement). The frequency of heart Tregs within the CD4$^+$ T cells gradually increased 7 days after MI, and maintained values until at least 28 days (Figure 1B). In contrast, the proportion of Tregs in the spleen and blood showed little variability over the time course (Figure 1B).

A similar accumulation of Tregs was also observed in hearts after myocardial ischemia/reperfusion injury (I/R injury). Tregs infiltrated into injured hearts within 1 day post-I/R injury, then peaked at day 3 and remained elevated until 7 days (Figure ID in the Data Supplement). The frequency of heart Tregs also reached a peak at day 3 after I/R injury, which was higher than that in blood and spleens (Figure 1C). In addition, the number of Tregs was also found increased in cryoinjured hearts. Tregs accumulated in the cryoinjured myocardium 1 day after injury and peaked at day 5 (Figure 1D). Taken together, these results indicate a possible role of heart Tregs after cardiac injury.

Transcriptome of Heart Tregs Has Unique Characteristics

To identify the transcriptional phenotype of heart Tregs, Tregs and Tconvs were isolated from hearts, spleens, and nondraining lymph nodes (NDLNs) 7 days after MI to perform RNA sequencing. Volcano plots revealed that the transcriptome of heart Tregs apparently differed from spleen or NDLN Tregs, whereas the latter 2 shared more similarities (Figure 2A). The differences between Tregs in hearts and lymphoid organs cannot be simply explained by different activation states in nonlymphoid tissue, because Treg activation signature[6,15] only accounted for a very small fraction of the distinguishing transcripts (Figure 2B and Figure IIA in the Data Supplement). Although heart Tregs exhibited a distinct transcriptome, they were clearly Tregs based on the expression of 79% of the canonical Treg signature,[5,6] including elevated expression of hallmark transcripts Foxp3, CD25, CTLA-4, and Klrg1 (Figure 2C).

Some upregulated differentially expressed genes in skin[8] and muscle[16] Tregs were also augmented in heart Tregs (Figure IIB in the Data Supplement). However, principal components analysis and transcriptomic analysis suggested transcriptional differences among these 3 tissue Tregs and between tissue Tregs and lymphoid organ Tregs[8,16] (Figure 2D and Figure IIB in the Data Supplement). Then we analyzed those upregulated differentially expressed genes in heart Tregs. The first group included *Ctla4, Areg*, and *Il1rl1*, which were also upregulated in muscle Tregs and skin Tregs. The second group was numerous cytokines, cytokine receptors, chemokines, and chemokine receptor–related genes (eg, *Il10*, *Il4ra*, *Ifngr1*, *Irf1*, *Tnf*, *Tnfrsf9*, *Ccr2*, *Ccr7*, *Ccr8*, *Ccrl2*, and *Cxcl10*). It is notable that a group of extracellular matrix organization– or collagen synthesis–related genes (eg, *Sparc*, *Dcn*, *Bgn*, *Mgp*, *Serpinh1*, *Postn*, *Col1a1*, *Col3a1*, and *Fn1*) were strikingly upregulated in heart Tregs (Figure 2E). Gene set enrichment analysis demonstrated that genes upregulated in heart Tregs displayed enrichment for Gene Ontology biological process terms involved in extracellular structure organization, extracellular matrix organization, collagen metabolic process, collagen biosynthetic process, wound healing, and regulation of smooth muscle cell proliferation, which were related to tissue repair (Figure 2F, Tables II and III in the Data Supplement).

To address whether the altered genetic signatures in heart Tregs are attributable to in situ microenvironment of cardiac injury, we compared the transcriptome of heart Tregs with heart-draining mediastinal lymph node (MLN) Tregs 7 days after MI. Volcano plots and principal components analysis revealed that the transcriptome of heart Tregs also apparently differed from MLN Tregs (Figure IIC in the Data Supplement and Figure 2D). The upregulated genes of heart Tregs and Gene Ontology biological process terms of heart Tregs mentioned earlier also significantly upregulated in heart Tregs in comparison with MLN Tregs (Figure 2E, Figure IIB and IID in the Data Supplement).

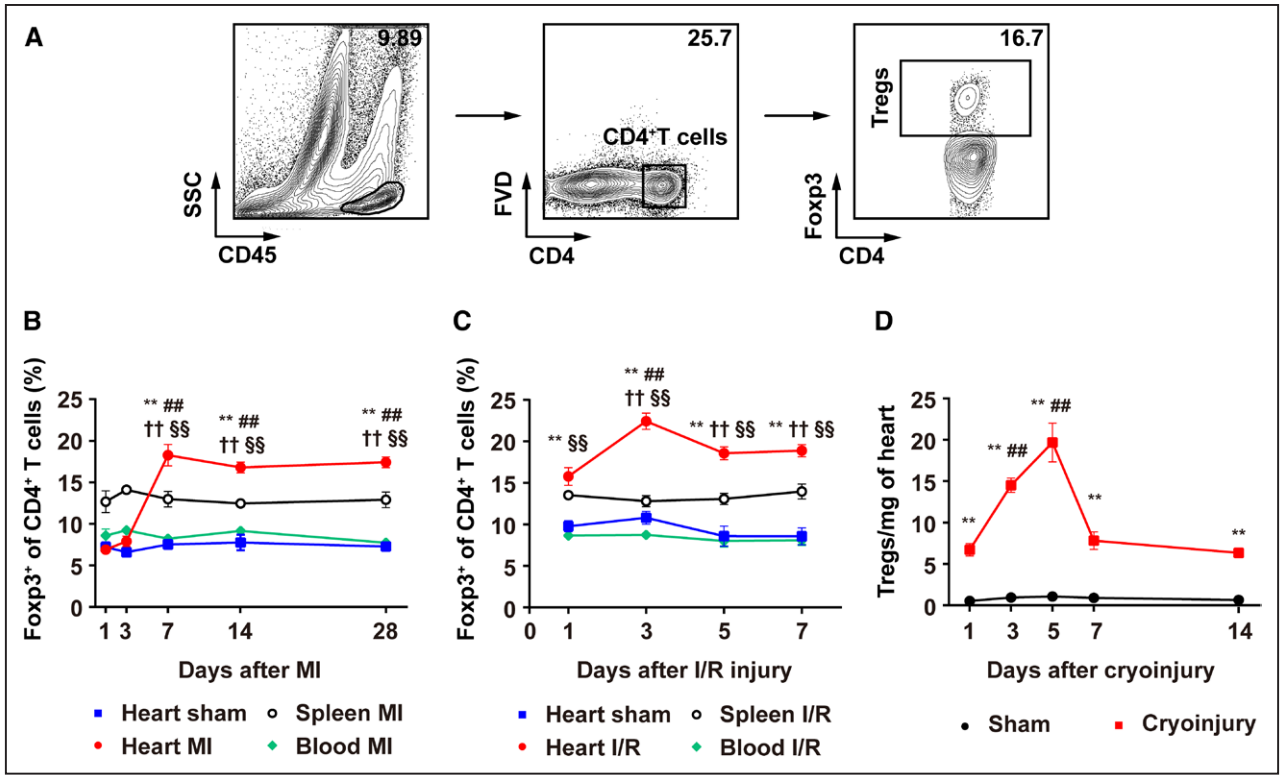

Figure 1. Treg accumulation in the injured myocardium.
A, Gating strategy for Foxp3+ Tregs in the hearts. **B**, The proportions of Tregs in the hearts, spleens, and peripheral blood at day 1, day 3, day 7, day 14, and day 28 after MI or sham operation. n=5 per group. **C**, The proportions of Tregs in the hearts, spleens, and peripheral blood at day 1, day 3, day 5, and day 7 after I/R injury or sham operation. n=5 per group. **D**, The numbers of Tregs in the hearts at day 1, day 3, day 5, day 7, and day 14 after cryoinjury or sham operation. n= 5per group. Statistical comparisons: 2-way ANOVA and the Tukey post hoc test were performed in **B** through **D**. ***P*<0.01 vs sham-operated hearts at each time point. ##*P*<0.01 vs 1 day post-MI hearts in **B**, 1 day post-I/R injury hearts in **C**, or 1 day postcryoinjury hearts in **D**. ††*P*<0.01 vs spleens at each time point in **B** and **C**. §§*P*<0.01 vs peripheral blood at each time point in **B** and **C**. CD indicates cluster of differentiation; FVD, fixable viability dye; I/R injury, myocardial ischemia/reperfusion injury; MI, myocardial infarction; SSC, side scatter; and Tregs, regulatory T cells.

To identify the transcriptional characteristics of heart Tregs in I/R injury, Tregs were isolated from hearts, spleens, and MLNs 3 days after I/R injury to perform RNA sequencing. Principal components analysis and volcano plots showed that the transcriptome of heart Tregs significantly differed from spleen or MLN Tregs (Figure 2D, Figure IIE and IIG in the Data Supplement). Gene set enrichment analysis showed that genes involved in extracellular matrix organization and extracellular structure organization, which are related to tissue repair, were significantly upregulated in heart Tregs in comparison with spleen or MLN Tregs (Figure IIF and IIH in the Data Supplement).Through principal components analysis and transcriptomic analysis, we found that heart Tregs from 2 models shared very similar transcriptome (Figure 2D and Figure IIB in the Data Supplement). In summary, our data suggest heart Tregs are a novel population of tissue Tregs, potentially involved in cardiac repair.

Heart Tregs Are Mainly Derived From the Circulating Compartment After MI

To identify the sources of heart Tregs after MI, we first asked whether the circulating Treg pool contributed to the accumulation of heart Tregs. Mice were treated with FTY720, an S1P1 receptor agonist that retains lymphocytes in secondary lymphoid tissue.[17] Under the treatment with FTY720, both the numbers and proportions of Tregs recruited to ischemic hearts markedly dropped on day 3 and day 7 after MI, whereas the number of CD4+T cells infiltrating into infarcted hearts also showed a significant decrease (Figure 3A). These results indicate that the accumulation of heart Tregs after MI may depend on the circulating Treg pool.

Therefore, a series of experiments were conducted to evaluate the ability of Tregs to infiltrate into the infarcted myocardium from circulation after MI. First, the kikGR/B6-ROSA transgenic mice were used to track the migration of Tregs and Tconvs. We exposed cervical lymph nodes of kikGR mice to violet light 3 days after MI, and tracked the Kikume-red+ Tregs and Tconvs from the cervical lymph nodes to the axillary lymph nodes, MLNs, and hearts 4 days after photoconversion (Figure 3B). Kikume-red+ Tregs and Tconvs emigrated from the cervical lymph nodes in mice, and the frequency of photo-converted cells within the Tregs or Tconvs were measured in the hearts, MLNs, and axillary lymph nodes (Figure 3C and 3D and Figure IIIA in

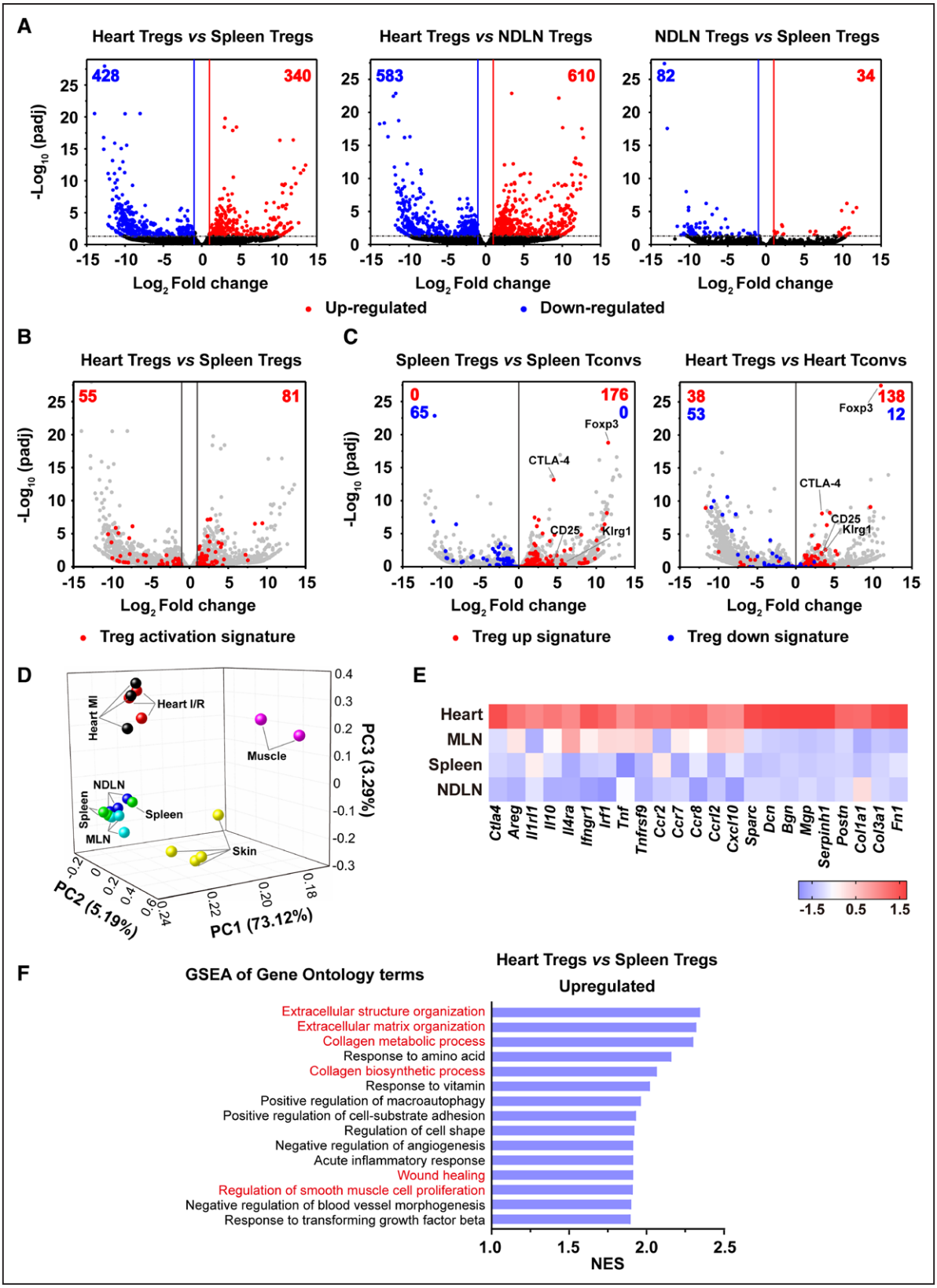

Figure 2. Distinct transcriptome of heart Tregs.

A, Tregs were sorted from the hearts, spleens, and NDLNs of Foxp3^{GFP} mice 7 days after MI. Volcano plots represent gene expression comparing heart Tregs vs spleen Tregs (**Left**), heart Tregs vs NDLN Tregs (**Center**), and NDLN Tregs vs spleen Tregs (**Right**). The numbers in the graph reveal the number of differentially expressed genes that differentially expressed >2-fold and with adjust *P* value (padj) <0.05. Upregulated and downregulated differentially expressed genes are highlighted in red or blue, respectively. Averaged from 3 experiments. **B**, Volcano plots represent gene expression comparing heart Tregs vs spleen Tregs 7 days after MI, and differentially expressed genes related to the Treg activation signature are highlighted in red. (*Continued*)

Figure 2 Continued. The numbers in the graph reveal the number of Treg activation signature genes differentially expressed in the set. Averaged from 3 experiments. **C**, Volcano plots represent gene expression comparing spleen Tregs vs Tconvs (**Left**) and heart Tregs vs Tconvs (**Right**) 7 days post-MI. Upregulated and downregulated Treg signature genes are highlighted in red or blue, respectively. The numbers in the graph represent the number of differentially expressed Treg signature genes. Averaged from 3 experiments. **D**, Principal components analysis of the transcriptome analysis of nonlymphoid tissue Tregs from the post-MI hearts, post-I/R injury hearts, muscles, skins, and lymphoid organ Tregs from the spleens, NDLNs and heart-draining MLNs after MI. The published RNA-sequencing data for muscle Tregs and skin Tregs were obtained from the Gene Expression Omnibus database (muscle Tregs, GSE76733; skin Tregs, GSE76138). Each plot represents 1 sort of pooled Tregs from mice as indicated in the graph. The distance of the dots indicates the similarity of the transcriptome: the greater the difference between the transcriptomes of Tregs, the greater the distance between the dots. **E**, Heat map of a selected list of differentially expressed transcripts among heart, heart-draining MLN, spleen, and NDLN Tregs. Averaged from 3 experiments. **F**, GSEA revealing Gene Ontology enrichment of the biological process category in the heart Tregs vs spleen Tregs 7 days after MI. The top 15 pathways are presented and ranked by the NES. Sets are listed only if padj <0.05. Averaged from 3 experiments. GSEA indicates gene set enrichment analysis; I/R, myocardial ischemia/reperfusion; MI, myocardial infarction; MLN, mediastinal lymph node; NDLN, nondraining lymph node; NES, normalized enrichment score; PC, principal component; Tconvs, conventional T cells; and Tregs, regulatory T cells.

the Data Supplement). When the fractions of Kikumered$^+$ cells in hearts and MLNs were normalized to that in axillary lymph nodes to calculate a migration ratio, Tregs manifested more effective migration to ischemic hearts than Tconvs, whereas no significant difference in migration between Tregs and Tconvs was observed in MLNs (Figure 3E).

Next, for detailed analysis of the contribution of the circulating Treg pool to heart Tregs, we performed a parabiosis experiment. We conjoined CD45.1 and CD45.2 mice for 2 weeks to establish a shared circulation.[18] Then, coronary ligation was performed on the CD45.1 parabiont, and the chimerism of Tregs was examined 7 days post-MI (Figure 3F and 3G). Chimerism of the heart Tregs was comparable to the admixture of the blood Tregs (Figure 3H, Left). Based on these data, we estimated that the recruitment of Tregs from the circulation accounted for nearly 95% of the Tregs within the infarcted hearts (Figure 3H, Right, and Figure IIIB in the Data Supplement). Our results collectively suggest that the accumulation of Tregs in the post-MI hearts mainly depends on recruitment from the circulating Treg pool.

Heart Tregs Are Clonally Expanded That Display a Unique T-Cell Receptor Repertoire

In addition to influx from the circulation, proliferation may contribute to the rapid accumulation of heart Tregs after MI. To address this possibility, we stained Tregs with Ki67. We found that ≈75% of heart Tregs 7 days after MI were Ki67-positive, much higher than those in spleen or NDLN Tregs (Figure 4A). In addition, we performed a proliferation assay by using 5-ethynyl-2′-deoxyuridine (EdU) incorporation. We detected ≈25% EdU$^+$ cells among heart Tregs, but a lower fraction within spleen or NDLN Tregs (Figure 4B). The fractions of Ki67$^+$ and EdU$^+$ cells within heart Tconvs were also increased in comparison with lymphoid organ Tconvs, but lower than those in heart Tregs (Figure 4A and 4B). These findings indicate a higher proliferation rate of heart Tregs than Tconvs and lymphoid organ Tregs post-MI.

To identify the clonality of the Tregs expanding in hearts post-MI, we applied paired single-cell RNA and T-cell receptor (TCR) sequencing of CD4$^+$ T cells from 7-day post-MI hearts and paired spleens to study their TCR repertoires. Unsupervised clustering was performed by Seurat,[19,20] and the *t*-distributed stochastic neighbor-embedding approach[21] was used to visualize clustering maps of heart and spleen CD4$^+$ T cells (Figure 4C and 4D). The clusters of heart Tregs and spleen Tregs were identified by expression of *Foxp3* (Figure 4C and 4D, Figure IVA and IVB in the Data Supplement). The characteristics of clonal restriction in heart Tregs were investigated by analyzing the TCR repertoires. A considerable fraction of heart Tregs was clonally expanded (Figure 4E, Left, and Figure IVC in the Data Supplement). In contrast, the spleen Tregs showed a much lower frequency of clonal expansion (Figure 4E, Right), and there were just a few TCR sequences shared between spleen Tregs and heart Tregs (Figure 4F). These results prove a unique TCR repertoire of heart Tregs and their local clonal expansion in the infarcted hearts after MI.

Conversion of Tconvs Makes a Small Contribution to Heart Treg Pool

Previous studies have shown that thymus-derived Tregs made up the majority of Tregs in secondary lymphoid organs. Some Tconvs can gain stable Foxp3 expression in the peripheral sites and can be converted to peripheral Tregs (pTregs).[22,23]

First, we examined the expression of Helios and Nrp-1 (neuropilin 1) on heart Tregs 7 days post-MI, because these markers are considered to distinguish between thymus-derived Tregs and pTregs.[23,24] Most heart Tregs showed a thymic origin with the Helios^{hi}Nrp-1^{hi} phenotype, similar to spleen or NDLN Tregs, indicating that the heart Tregs were mainly thymus derived (Figure 5A).

To directly identify whether Tconvs can be converted to heart Tregs post-MI, CD45.2$^+$ Tconvs were isolated and adoptively transferred into CD45.1 mice soon after MI. Donor-derived Tconvs (CD45.2$^+$CD4$^+$Foxp3$^-$) could be detected in organs 2 weeks after Tconvs adoptive transfer (Figure VA in the Data Supplement). It is surprising that a small population of donor-derived pTregs (CD45.2$^+$CD4$^+$Foxp3$^+$) was detected not only in the lymphoid organs, but also in the infarcted hearts. Moreover, donor-derived pTregs showed an even higher

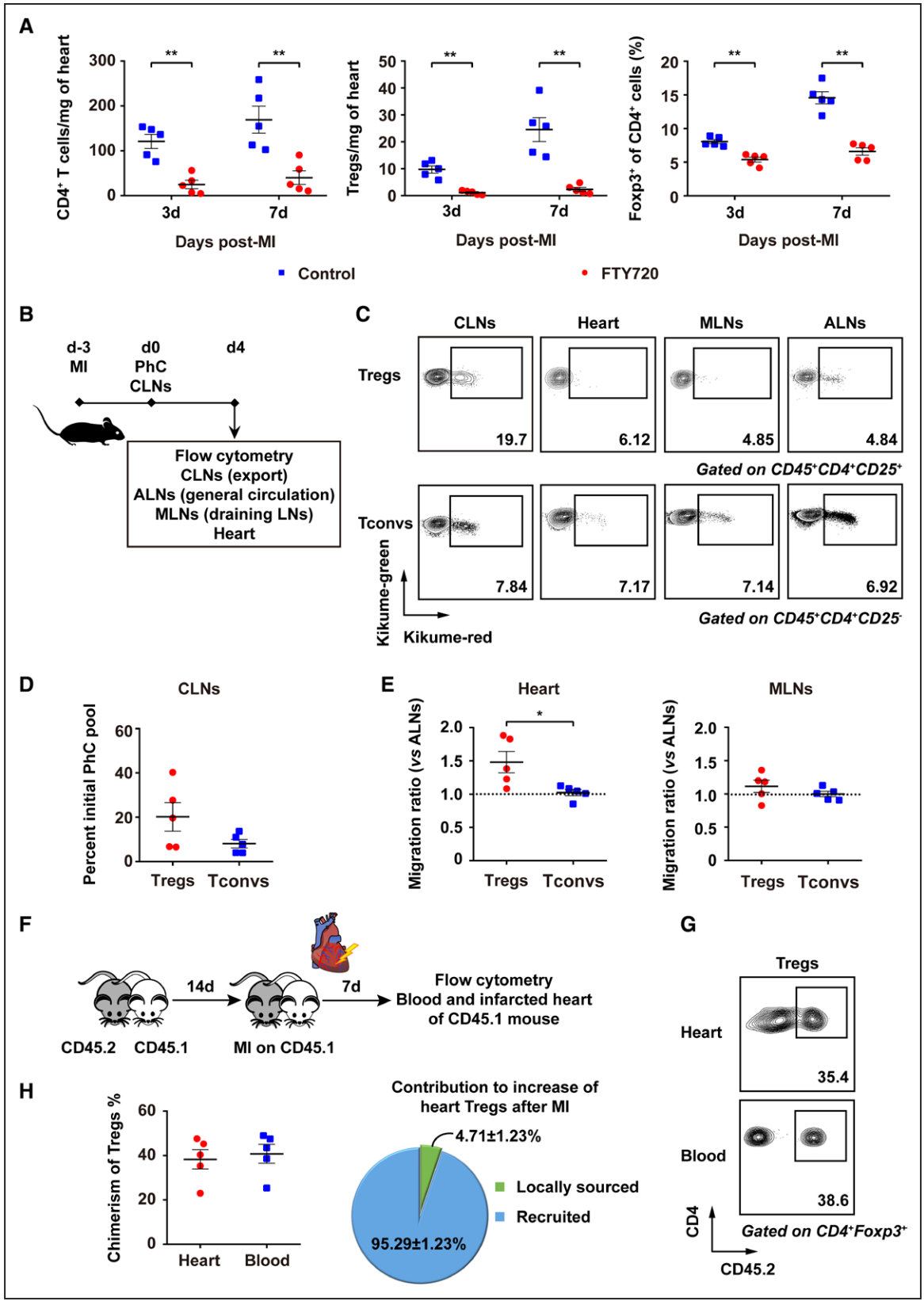

Figure 3. Heart Tregs depend on the circulating pool.

A, FTY720 or vehicle was administrated 1 day before MI and every day after operation. The numbers or fractions of heart CD4⁺ T cells and Foxp3⁺ Tregs were measured by using flow cytometry 3 or 7 days after MI. n=5 per group. **B**, Diagram of the experimental protocol. The kikGR mice were subjected to MI. After 3 days, the CLNs were exposed to violet light noninvasively. Tregs or Tconvs from the indicated tissues were examined by flow cytometry to track Kikume-red⁺ photo-converted (PhC) cells 4 days later. **C**, Representative flow cytometry analysis of Kikume-red⁺ PhC Tregs (**Top**) and Tconvs (**Bottom**) in the CLNs, hearts, MLNs, and ALNs. Numbers indicate the proportion of cells in the frame. **D**, Exodus from the PhC CLN pool. (*Continued*)

Figure 3 Continued. **E**, The migration ratio is the percentage of Kikume-red$^+$ cells in the hearts or MLNs normalized to those in the ALNs (general circulation). n=5 per group. **F**, Parabiosis experiments of CD45.1 and CD45.2 mice. CD45.1 and CD45.2 mice were conjoined for 2 weeks. Then the CD45.1 parabiont was subjected to MI. Chimerism was examined 7 days post-MI. **G**, Representative flow cytometry graphs of the chimerism of Tregs in the hearts (**Top**) and peripheral blood (**Bottom**). Numbers indicate the proportion of cells in the frame. **H**, Summary data for the quantification of chimerism for Tregs in the peripheral blood and hearts (**Left**). Relative contribution of recruited Tregs vs locally sourced Tregs to the total heart Treg population 7 days after MI (**Right**). n=5 per group. Statistical comparisons: 2-tailed unpaired *t* test was performed in **A**, **D**, and **E**. **P*<0.05, ***P*<0.01. ALNs indicates axial lymph nodes; CD, cluster of differentiation; CLNs, cervical lymph nodes; LNs, lymph nodes; MI, myocardial infarction; MLNs, mediastinal lymph nodes; Tconvs, conventional T cells; and Tregs, regulatory T cells.

frequency in the infarcted hearts than in the spleens and NDLNs (Figure 5B).

Finally, we analyzed the TCR repertoires of heart Tconvs after MI. When comparing the TCR repertoires of heart Tregs and heart Tconvs, identical TCR clonotypes were found, indicating a probable contribution of the conversion of Tconvs to the heart Tregs (Figure 5C and Figure VB in the Data Supplement).

Interleukin-33/ST2 Axis Governs Accumulation and Expansion of Heart Tregs

Next, we set up to determine the mechanism of heart Treg accumulation after MI. We noticed that *Il1r1l*, which encodes ST2 (suppression of tumorigenicity 2), the receptor of interleukin-33 (IL-33), was strongly upregulated in heart Tregs, and the increased transcript level was further confirmed by RT-PCR (Figures 2E and 6A and 6B). Considering that IL-33 is related to Treg homeostasis in parenchymal tissues,[16,25,26] we hypothesized that heart Tregs might accumulate and expand in response to IL-33.

Flow cytometry was performed to measure ST2 protein. The percentage of ST2$^+$ Tregs within heart Tregs was much higher than spleen Tregs, and the fraction of ST2$^+$ heart Tregs elevated at day 3 and sustained until at least 28 days (Figure 6C and Figure VIA in the Data Supplement). Moreover, we found that both *Il33* transcript and IL-33 protein levels were increased after MI, peaking at day 5 (Figure 6D and 6E). To pinpoint the cellular source of IL-33 in the infarcted hearts, we sorted the CD45$^+$ and CD45$^-$ cell fractions from the hearts 5 days post-MI and quantified their *Il33* transcript levels, and found that IL-33 was mainly expressed by CD45$^-$ cells (Figure VIB in the Data Supplement). Next, we sorted endothelial cells, cardiomyocytes, and cardiac fibroblasts from the post-MI hearts and quantified their *Il33* transcript levels. Results showed that IL-33 was highly expressed in cardiac fibroblasts, and cardiomyocytes also expressed a small amount of IL-33, but endothelial cells hardly showed any expression (Figure 6F). Then immunofluorescence staining was used to confirm the cell source of IL-33, which indicated that the majority of IL-33–positive cells was Vimentin$^+$ fibroblasts, except in rare cases were α-actinin$^+$ cardiomyocytes, but none of them were costained with CD31, suggesting that the main source was cardiac fibroblasts, which was consistent with a previous study[27] (Figure 6G, Figure VIC and VID in the Data Supplement).

Then we performed a series of loss- and gain-of-function experiments to evaluate the function of the IL-33/ST2 axis in the accumulation of heart Tregs after MI. The number of heart Tregs was markedly reduced in *Il1rl1*$^{-/-}$ mice in comparison with wild-type mice 7 days after MI, whereas there were no obvious changes in spleen Tregs (Figure 6H). In contrast, administration of recombinant IL-33 induced an impressive expansion of heart Tregs 7 days post-MI, because the numbers and proportions of heart Tregs were markedly increased in IL-33–treated mice (Figure 6I and Figure VIE in the Data Supplement). IL-33 administration also elevated the proportions of proliferating heart Tregs (Ki67$^+$CD4$^+$Foxp3$^+$) and ST2-positive heart Tregs (ST2$^+$CD4$^+$Foxp3$^+$; Figure VIF in the Data Supplement). Besides, the spleen Tregs were also expanded and expressed ST2 and Ki67 more often under IL-33 treatment relative to phosphate-buffered saline treatment (Figure 6I and Figure VIF in the Data Supplement). These observations suggest that the IL-33/ST2 axis induces the heart Treg expansion by promoting their proliferation.

Heart Tregs Overexpressing Sparc Ameliorate Survival and Protect Against Rupture After MI

Previous studies suggest a reparative role of Tregs in myocardial healing after MI.[12–14] Tregs indeed perform anti-inflammatory activities after MI, whereas their tissue-distinct capacity to directly influence pathological processes within the infarcted hearts has not been fully elucidated.

In an attempt to further delineate the mechanisms by which heart Tregs promote tissue repair after MI, we analyzed the transcriptome of heart Tregs and noticed that *Sparc* was among the highest differentially expressed genes of heart Tregs (Figure 7A and Figure VIIA in the Data Supplement). Sparc (secreted acidic cysteine-rich glycoprotein, also known as osteonectin), a collagen-binding matricellular protein, plays a pivotal role in collagen assembly into the extracellular matrix and has been reported to play a crucial role in preserving ventricular integrity after MI.[28] The higher transcript level of *Sparc* in heart Tregs was further confirmed by RT-PCR (Figure 7B). Moreover, IL-33 treatment could induce upregulation of *Sparc* expression in heart Tregs (Figure 7C).

To functionally determine whether Sparc plays a role in heart Treg-mediated tissue repair post-MI, we

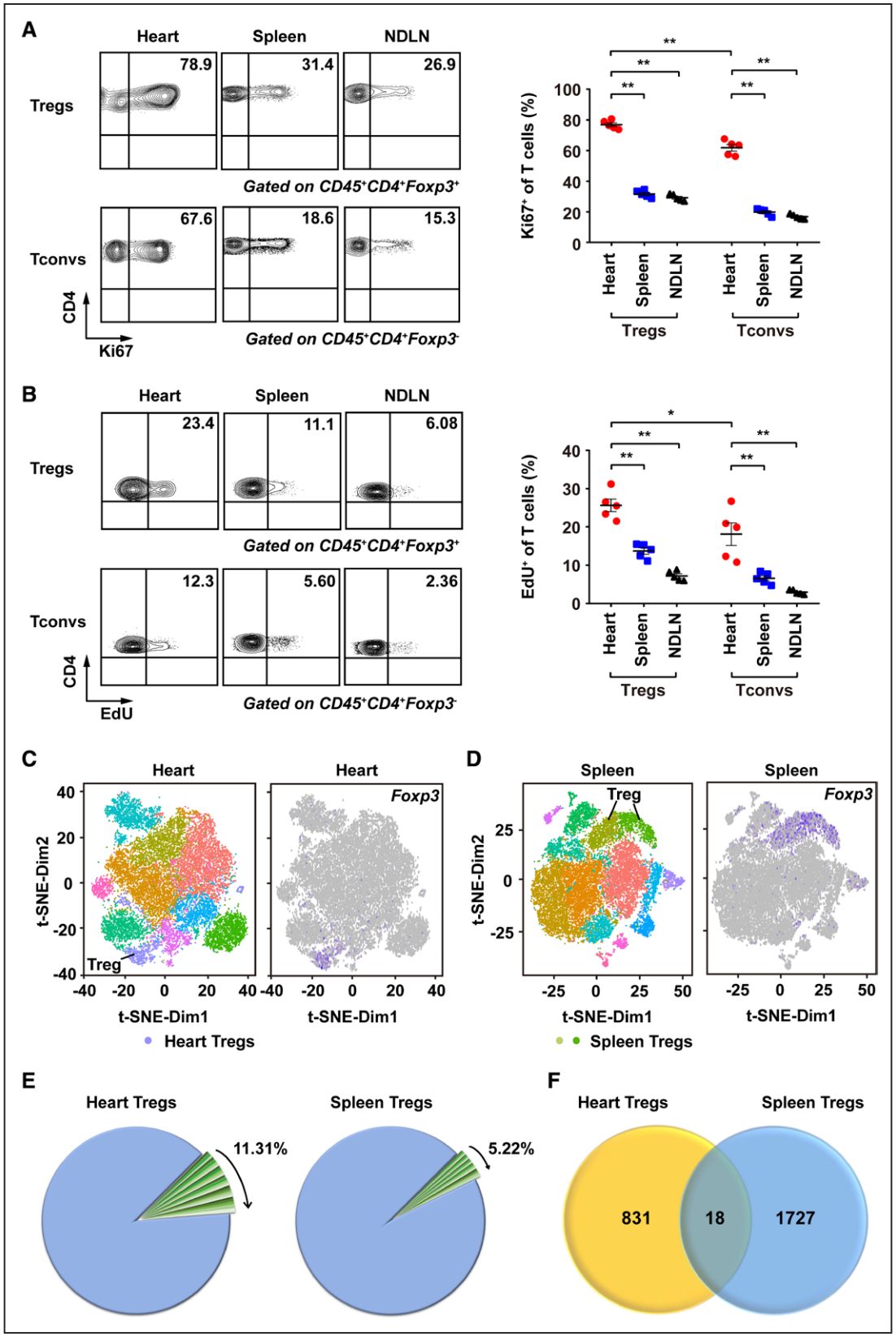

Figure 4. Heart Tregs are clonally expanded.

A, Proportion of Tregs and Tconvs in the cell cycle 7 days post-MI. Ki67 expression of Tregs and Tconvs in the hearts, spleens, and NDLNs was detected by flow cytometry 7 days after MI. **Left**, Representative flow cytometry graphs. Numbers indicate the proportion of cells in the frame. **Right**, Summary data. n=5 per group. **B**, Degree of Treg and Tconv proliferation 7 days post-MI. Mice were treated with EdU at day 6 post-MI, and then the proliferation of Tregs and Tconvs in the hearts, spleens, and NDLNs was detected by flow cytometry 7 days after MI. **Left**, Representative flow cytometry graphs. Numbers indicate the proportion of cells in the frame. **Right**, Summary data. n=5 per group. **C**, Single-cell RNA- and TCR-sequencing analysis of heart and (*Continued*)

Figure 4 Continued. spleen CD4+ T cells 7 days post-MI. **Left**, The t-SNE projection of 20755 heart CD4+ T cells shows 10 main cell clusters, including 1 cluster of heart Tregs. Each dot represents a single cell and each cluster is colored with a different color. **Right**, Expression levels of *Foxp3* across 20755 single heart CD4+ T cells were shown in the graph. **D**, **Left**, The t-SNE projection of 23471 spleen CD4+ T cells shows 14 main clusters, including 2 clusters of spleen Tregs. Each dot represents a single cell and each cluster is colored with a different color. **Right**, Expression levels of *Foxp3* across 23471 single spleen CD4+ T cells were shown in graph. **E**, TCRα and TCRβ sequences for heart Tregs (**Left**) and spleen Tregs (**Right**). Identical TCR clonotypes are presented in blue. Repeated TCR clonotypes are presented in green, and the width of each slice in the pie chart represents the fraction of a clonotype's repeat. Numbers in the top right of the pie charts represent total proportion of the repeated clonotypes. **F**, Venn diagram shows the overlap of TCR clonotypes between heart Tregs and spleen Tregs. Statistical comparisons: 2-way ANOVA and Tukey post hoc test were performed in **A** and **B**. **P*<0.05, ***P*<0.01. CD indicates cluster of differentiation; EdU, 5-ethynyl-2′-deoxyuridine; MI, myocardial infarction; NDLN, nondraining lymph node; Tconvs, conventional T cells; TCR, T-cell receptor; Tregs, regulatory T cells; and t-SNE, t-distributed stochastic neighbor embedding.

applied anti-CD25 antibody to deplete Tregs and administered a replication-deficient adenovirus harboring mouse *Sparc* (Ad-Sparc) to overexpress Sparc globally. Control adenovirus (Ad-Ctrl) was used as control (Figure VIIB in the Data Supplement). In the anti-CD25–treated groups, CD4+CD25+Foxp3+ Tregs presented a significantly reduced fraction in peripheral blood relative to the isotype control antibody immunoglobulin (Ig) G–treated group (Figure VIIC in the Data Supplement). Overexpression of Sparc in the infarcted hearts was identified 7 days and 14 days post-MI in the Ad-Sparc administration groups in comparison with Ad-Ctrl groups (Figure VIID in the Data Supplement). In comparison with Ad-Ctrl–treated Treg-ablated mice, the Ad-Sparc–treated Treg-ablated mice had significantly improved survival, attributing to fewer cardiac ruptures after MI (Figure 7D and 7E). In contrast, a difference in survival was not observed between Ad-Sparc–treated Treg-ablated mice and IgG+Ad-Ctrl–treated mice, indicating a near-complete rescue by Ad-Sparc (Figure 7D and 7E). Echocardiography was performed 14 days post-MI in surviving mice, and there were no statistically significant differences among those treatment groups (Figure 7F). No improvement of cardiac function was found after Sparc overexpression, which could presumably be explained by better survival of mice with poor cardiac function in the Ad-Sparc–treated group than in the Ad-Ctrl–treated group.

We next focused on scar formation of the infarct zone. Although the scar size did not significantly differ among these treatments (Figure VIIIA and VIIIB in the Data Supplement), the infarct thickness was increased in Ad-Sparc–treated Treg-ablated mice in comparison with that in the Ad-Ctrl–treated Treg-ablated group, which was consistent with the result of lower cardiac ruptures because a thick scar was not prone to rupture[29] (Figure VIIIA and VIIIC in the Data Supplement). Because collagen is the most abundant structural component of infarct scar tissue, the collagen content and maturation were analyzed after MI. First, Treg depletion reduced the Sirius red–stained collagen content of the infarct zone, and collagen III, as well, but not collagen I expression, whereas Sparc overexpression reversed these effects (Figure VIIID in the Data Supplement and Figure 8A through 8D). Because myofibroblast was the main producer of collagen in hearts after MI,[30,31] we further assessed the α-smooth muscle actin expression, but found no difference among these groups (Figure 8B). Next, as for collagen maturation, Sirius red polarization microscopy revealed a predominance of thicker tightly packed (orange-red) collagen fibers within infarct scars in Ad-Sparc–treated Treg-ablated mice or isotype control IgG-treated mice than in control Ad-Ctrl–treated Treg-ablated mice, indicating a remedy of collagen maturation by Sparc overexpression after Treg depletion (Figure 8E). Moreover, analysis of the collagen maturation by electron microscopy revealed that Treg depletion resulted in loose, disturbed, and thinner collagen fibers in the infarct scars, whereas collagen fiber organization was tight and parallel, and the diameter of collagen fibers was larger after Sparc overexpression, which also indicated improved collagen maturation (Figure 8F and Figure VIIIE in the Data Supplement).

To further validate that Sparc was one of the important functional molecules in heart Tregs, we conducted in vitro experiments. Because tissue Tregs can hardly survive in vitro as previously described,[5] we sorted spleen Tregs and overexpressed Sparc by Sparc-overexpressing lentivirus, and the overexpression was confirmed by RT-PCR (Figure VIIIF in the Data Supplement). We cocultured the cardiac fibroblasts with Tregs and found that cardiac fibroblasts that were cocultured with Sparc-overexpressing Tregs expressed a higher level of *Col3a1* than cardiac fibroblasts that were cocultured with control Tregs or cultured alone (Figure 8G). In contrast, *Col1a1* and *ASMA* did not show obvious differences (Figure 8G). Taken together, heart Tregs lead to increased collagen content and enhanced maturation in the infarct scars, and Sparc is critical in this process.

DISCUSSION

Emerging evidence has recently established that tissue Tregs have multiple functions beyond their initial immunosuppressive effect within a variety of tissues.[3–10] Here, we identified that Tregs accumulated in infarcted hearts, with a distinctive transcriptome, represented a unique population of tissue Tregs. Heart Tregs were mainly recruited from circulation, whereas local expansion and conversion also contributed to the compartment. The IL-33/ST2 axis was important for expanding heart Tregs. Moreover, we focused on their direct ability of wound repair as suggested by transcriptomic data

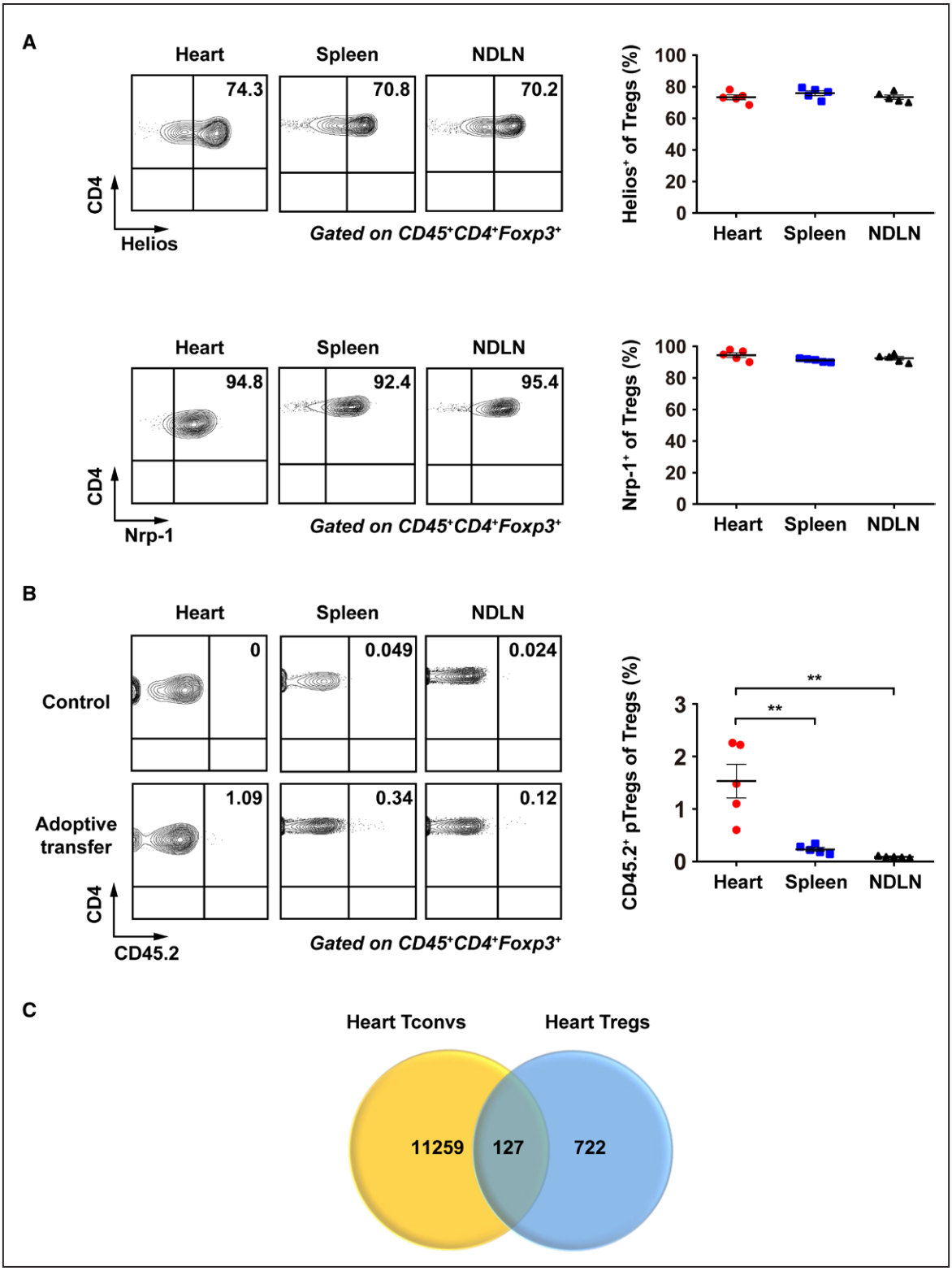

Figure 5. A small contribution of the conversion of Tconvs to heart Tregs.
A, **Left**, Representative flow cytometry analysis of Helios (**Top**) or Nrp-1 (**Bottom**) expression of Tregs in the hearts, spleens, and NDLNs of mice 7 days after myocardial infarction. Numbers indicate the proportion of cells in the gate. **Right**, Summary data for the proportion of Helios (**Top**) or Nrp-1 (**Bottom**) expression of Tregs in the hearts, spleens, and NDLNs. n =5 per group. **B**, Adoptive transfer experiments. Foxp3^{-} Tconvs were sorted from the spleens of CD45.2^{+}Foxp3^{GFP} mice and transferred into CD45.1^{+} recipients soon after a myocardial infarction. Then Treg compartments were detected 2 weeks after adoptive transfer. **Left**, Representative flow cytometry analysis of donor-derived pTregs in the hearts, spleens, and NDLNs of mice adoptive transferred with donor Tconvs or phosphate-buffered saline as a control. Numbers indicate the proportion of cells in the gate. **Right**, Summary data for donor pTreg percentage. n=5 per group. **C**, Venn diagram shows the overlap of T-cell receptor clonotypes between heart Tconvs and heart Tregs. Statistical comparisons: 1-way ANOVA with the Tukey multiple comparison test was performed in **A** and **B**. ** P<0.01. CD, cluster of differentiation; NDLN, nondraining lymph node; Nrp-1, neuropilin-1; pTregs, peripheral Tregs; Tconvs, conventional T cells; and Tregs, regulatory T cells.

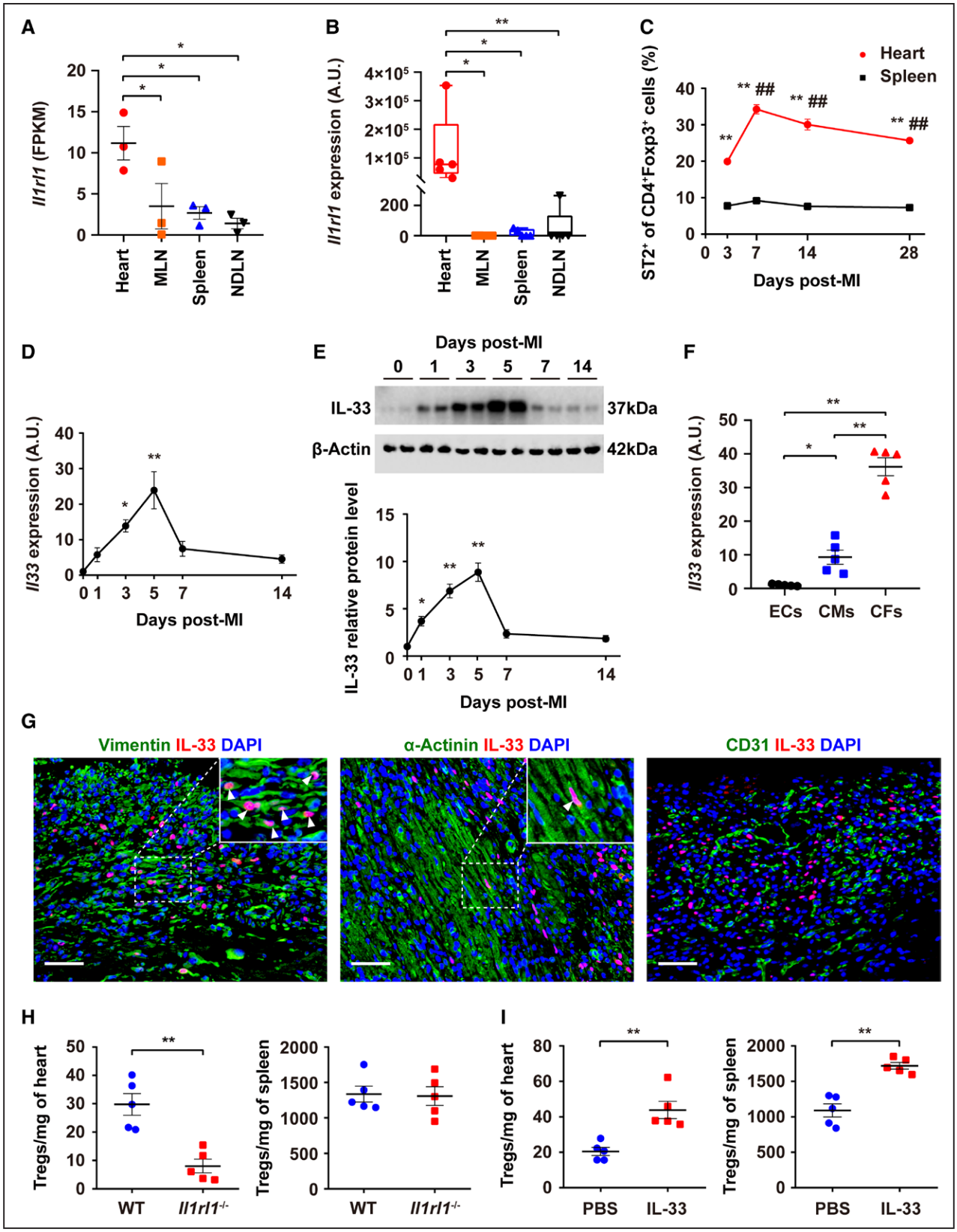

Figure 6. The IL-33/ST2 axis governs accumulation and expansion of heart Tregs.
A, FPKM of *Il1rl1* transcripts as quantified by RNA sequencing. n=3 per group. **B**, *Il1rl1* transcripts in isolated Tregs of hearts, MLNs, spleens, and NDLNs from Foxp3^{GFP} mice 7 days after MI were quantified by RT-PCR. n=5 per group. **C**, Summary data for the fraction of ST2$^+$ Tregs in the hearts and spleens at day 3, day 7, day 14, and day 28 after MI. n=5 per group. **D**, *Il33* transcripts in the infarcted myocardium were quantified by RT-PCR at day 0, day 1, day 3, day 5, day 7, and day 14 after MI. n=5 per group. **E**, IL-33 protein levels in the infarcted myocardium were quantified by Western blotting at day 0, day 1, day 3, day 5, day 7, and day 14 after MI. **Top**, Representative immunoblot. **Bottom**, summary data. n=5 per group. (*Continued*)

Figure 6 Continued. **F**, *Il33* transcripts in endothelial cells, cardiomyocytes, and cardiac fibroblasts isolated from infarcted hearts were quantified by RT-PCR 5 days after MI. n=5 per group. **G**, Representative immunofluorescence staining of IL-33 with Vimentin (**Left**), α-actinin (**Middle**), and CD31 (**Right**) in infarcted hearts 5 days after MI, cell nuclei were stained with DAPI. Scale bar, 50 μm. **H**, The numbers of Tregs in the hearts (**Left**) and spleens (**Right**) of WT and *Il1rl1*$^{-/-}$ mice 7 days post-MI. n=5 per group. **I**, The numbers of Tregs in the hearts (**Left**) and spleens (**Right**) of IL-33–treated and PBS-treated mice 7 days post-MI. n=5 per group. Statistical comparisons: 1-way ANOVA with the Tukey multiple comparison test was performed in **A** and **D** through **F**; nonparametric Kruskal-Wallis test was performed in **B**; 2-way ANOVA and Tukey post hoc test were performed in **C**; 2-tailed unpaired *t* test was performed in **H** and **I**. ***P*<0.01 vs spleens at each time point, ##*P*<0.01 vs 3 day post-MI hearts in **C**. **P*<0.05, ***P*<0.01 vs day 0 in **D** and **E**. **P*<0.05, ***P*<0.01 in **A**, **B**, **F**, **H**, and **I**. A.U. indicates arbitrary unit; CD, cluster of differentiation; CFs, cardiac fibroblasts; CMs, cardiomyocytes; DAPI, 4′,6-diamidino-2-phenylindole; ECs, endothelial cells; FPKM, fragments per kilobase of transcript per million fragments mapped; IL-33, interleukin-33; *Il1rl1*, interleukin 1 receptor like 1; MI, myocardial infarction; MLN, mediastinal lymph node; NDLN, nondraining lymph node; PBS, phosphate-buffered saline; RT-PCR, reverse transcription polymerase chain reaction; ST2, suppression of tumorigenicity 2; Tregs, regulatory T cells; and WT, wide type.

and identified Sparc as a functional mediator of heart Tregs to promote repair.

Tregs That Accumulate in the Injured Myocardium Have a Distinct Transcriptome

Based on the unique transcriptomic characteristics, we identified a previously unrecognized tissue-Treg population in hearts. The markedly altered transcripts in our transcriptome data, which first caught our attention, are genes encoding molecules related to Treg suppressive capacity. *Ctla-4* and *Klrg-1* were upregulated on heart Tregs, supporting the notion that heart Tregs may be endowed with especially strong inhibitory activity in the inflammatory microenvironment. More importantly, heart Tregs overexpressed extracellular matrix organization or collagen synthesis–related genes, distinguishing them from the lymphoid organ Tregs, whose products help them perform important functions in maintaining cardiac function and integrity after MI. Although the transcriptional profile has a certain degree of similarity, tissue Tregs are also highly complex and heterogeneous in different organs. These differences suggest that the microenvironment related to damage and specific tissues is critical in orchestrating Tregs. Heart Tregs in I/R injury models also have a prohealing phenotype similar to that of heart Tregs in MI models, probably because of the similar injured microenvironment in myocardium.

Previous studies indicate that CD4$^+$ T cells first become primed and proliferate in the heart-draining MLNs after MI, and then infiltrate into injured hearts. These findings raise an important question: Where do heart Tregs take on their distinctive phenotypes, MLNs, or hearts? To address it, we compared transcriptomic characteristics between heart Tregs and MLN Tregs. The transcriptomic data showed that, differently from MLN Tregs, heart Tregs displayed a distinct repertoire signature dominated by a prohealing phenotype, which was attributable to the myocardial milieu under the scenario of myocardial injury. A recently published study also consistently pinpoints that T cells infiltrating the infarcted myocardium display a unique repertoire signature and clonally expand in situ.[32] However, we also noticed that genes encoding Treg suppressive molecular *Ctla4* and some cytokines, cytokine receptors, chemokines, and chemokine receptors were upregulated in MLN Tregs in comparison with spleen and NDLN Tregs. Therefore, we conclude that heart Tregs comply with a pragmatic lymphocyte-trafficking paradigm in a way that Tregs become primed and proliferative in MLNs. More importantly, the injured myocardium imposes an activation context that promotes the development of heart Tregs poising to exhibit a cardioprotective phenotype during the healing stage. It is notable that a recent study provides valid evidence to demonstrate that tissue Tregs are initially priming in lymph nodes and give rise to fully mature tissue Tregs in nonlymphoid tissues, exactly supporting our conclusion.[33]

Heart Tregs Are Mainly Recruited From Circulation, Coupled With Proliferation and Conversion, and the IL-33/ST2 Axis Promotes Their Expansion

Tissue Tregs may have several different sources, including recruitment from peripheral Treg pool, amplification of recruited or locally colonized Tregs, and conversion from Tconvs.[25] Although some researchers have speculated that Tregs are mainly recruited from the peripheral circulation after MI,[12,13,34] relevant evidence is missing. Through FTY720 and photoconversion experiments, we confirmed the migration of circulating Tregs to the hearts after MI. More importantly, we calculated that 95% of the increased Treg population in the MI myocardium came from the peripheral circulation through parabiosis experiments. In comparison with lymphoid organs, the preferential aggregation of Tregs in the injured hearts may depend on their upregulated expression of chemokines and chemokine receptors as suggested by transcriptomic data.

In addition, it cannot be ignored that the other 2 processes also contributed to supplementing the Treg pool. Proliferative markers confirmed that heart Tregs exhibited heightened proliferation, which is consistent with visceral adipose tissue Tregs and muscle Tregs.[5,6,16,26] In particular, TCR repertoire data revealed that the clonal expansions of heart Tregs occurred in response to MI and were more pronounced in heart Tregs than in spleen Tregs, which suggests the possibility of specific antigen-TCR recognition by heart Tregs. Although heart Tregs expressed high levels of markers

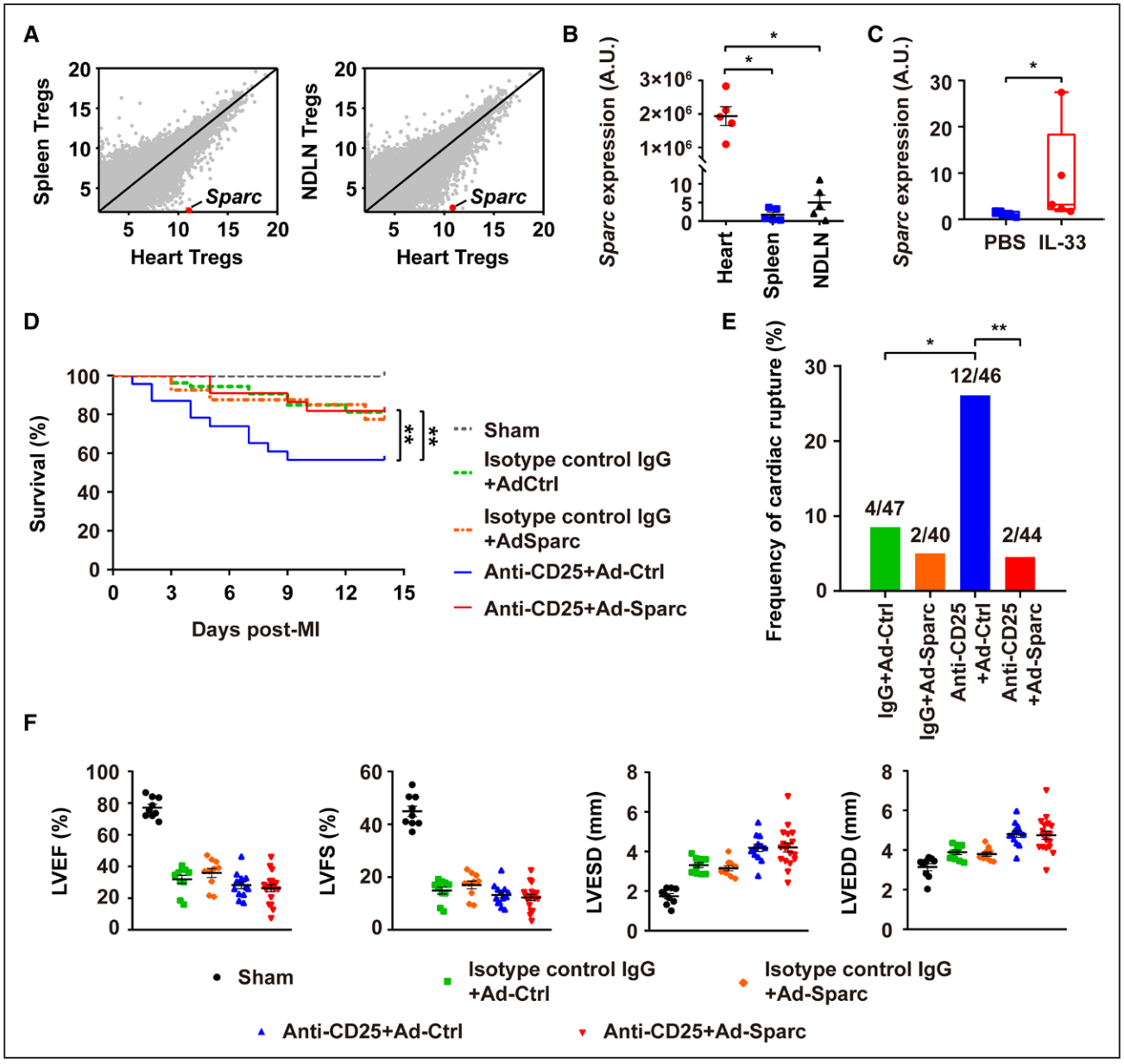

Figure 7. Heart Tregs overexpressing Sparc ameliorate survival and protect against rupture after MI.
A, Scatter plots comparing gene expression quantified by RNA sequencing of heart Tregs vs spleen Tregs (**Left**) and heart Tregs vs NDLN Tregs (**Right**). The *Sparc* gene is highlighted in red. Averaged from 3 experiments. **B**, *Sparc* transcripts in isolated Tregs of hearts, spleens, and NDLNs from Foxp3^{GFP} mice 7 days after MI were quantified by RT-PCR. n=5 per group. **C**, *Sparc* transcripts in isolated heart Tregs from IL-33–treated and PBS-treated mice 7 days after MI were quantified by RT-PCR. n=5 per group. **D**, Kaplan-Meier survival curve shows the survival of sham-operated mice, isotype control IgG+Ad-Ctrl–treated mice, isotype control IgG+Ad-Sparc–treated mice, Ad-Ctrl–treated Treg-ablated mice, and Ad-Sparc–treated Treg-ablated mice after MI. n=40 to 47 per group. **E**, Frequency of cardiac rupture among mice in the indicated groups. n=40 to 47 per group. **F**, Quantification of LVEF, LVFS, LVESD, and LVEDD by echocardiography at 14 days after MI among the indicated groups. n=9 to 18 per group. Statistical comparisons: 1-way ANOVA with the Tukey multiple comparison test was performed in **B** and **F**; nonparametric Mann-Whitney *U* test was performed in **C**; Kaplan-Meier method log-rank test was performed in **D**; Fisher exact test was performed in **E**. **P*<0.05, ***P*<0.01. Ad-Ctrl indicates control adenovirus; Ad-Sparc, secreted acidic cysteine-rich glycoprotein–overexpressing adenoviral vector; A.U., arbitrary unit; CD, cluster of differentiation; IgG, immunoglobulin G; IL-33, interleukin-33; LVEDD, left ventricular end-diastolic dimension; LVEF, left ventricular ejection fraction; LVESD, left ventricular end-systolic dimension; LVFS, left ventricular fractional shortening; MI, myocardial infarction; NDLN, nondraining lymph node; PBS, phosphate-buffered saline; RT-PCR, reverse transcription polymerase chain reaction; and Tregs, regulatory T cells.

of thymus-derived Tregs, our results suggested that a minor proportion of heart Tregs was converted from Tconvs. By using the heart-specific antigen transgenic mice, Rieckmann et al[32] also consistently found that Tconvs can be transformed into Tregs in MI. Otherwise, there was no conversion of visceral adipose tissue Tregs from Tconvs, indicating the distinct sources of individual tissue Tregs.[26]

Given the strongly upregulated expression of ST2 on heart Tregs, we speculated that IL-33 drove heart Tregs enrichment. As expected, we verified that the IL-33/ST2 axis played an important role in the accumulation of

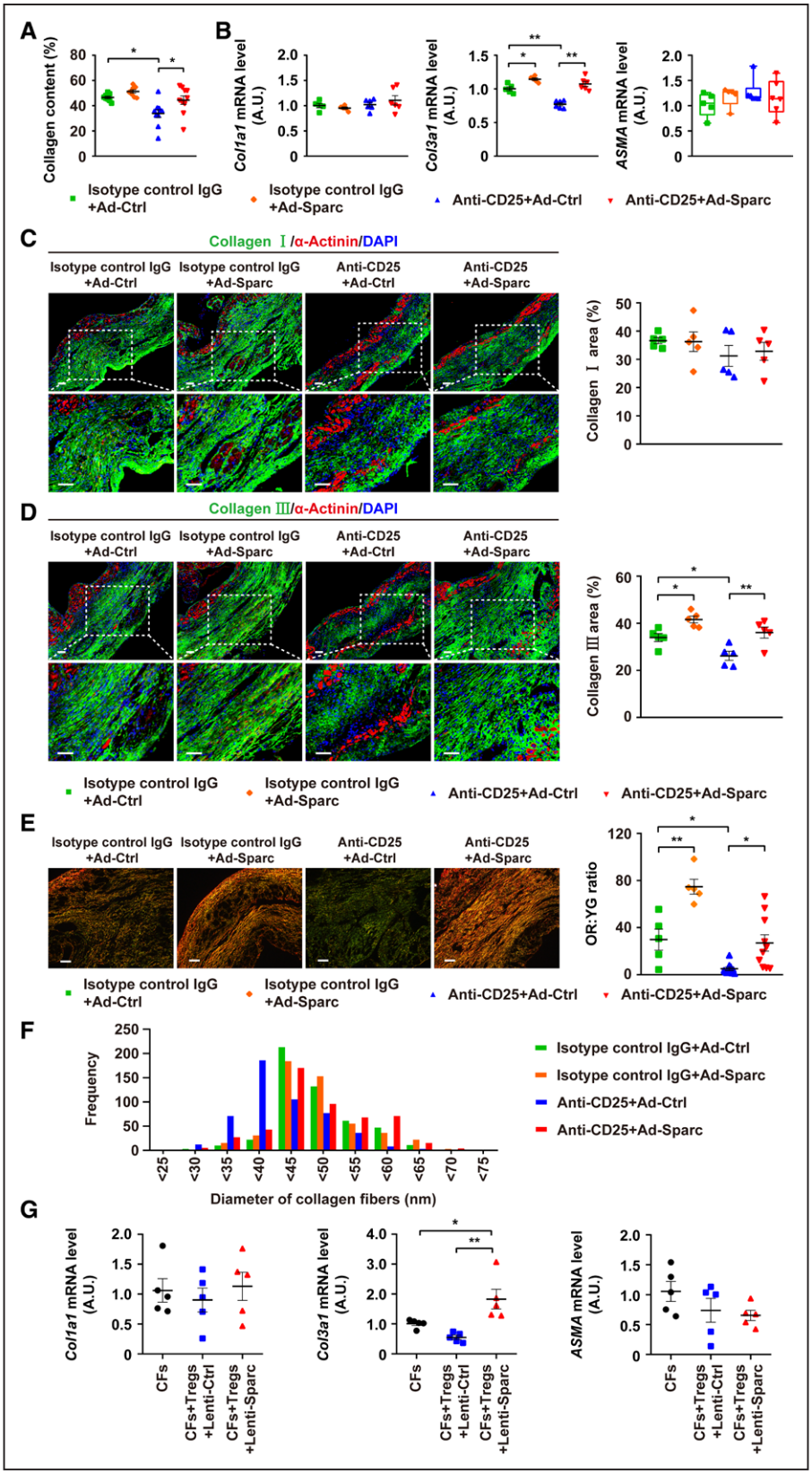

Figure 8. Heart Tregs overexpressing Sparc protect against cardiac rupture through increasing collagen content and enhancing maturation in infarct scars.

A, Quantification of collagen content in the infarct zone among the indicated groups. n=8 to 10 per group. **B**, RT-PCR analysis of *Col1a1*, *Col3a1*, and *ASMA* mRNA expression in the infarct zone among the indicated groups 5 days post-MI. n=5 to 6 per group. **C**, **Left**, Representative immunofluorescence staining of collagen I (green) and α-actinin (red) of the infarct zone in infarcted hearts 14 days after MI. Scale bar, 50 μm. **Right**, Summary data for the collagen I expression among the indicated groups. n=5 per group. **D**, **Left**, Representative immunofluorescence staining of collagen III (green) and α-actinin (*Continued*)

Figure 8 Continued. (red) of the infarct zone in infarcted hearts 14 days after MI. Scale bar, 50 μm. **Right**, Summary data for the collagen III expression among the indicated groups. n=5 per group. **E**, **Left**, Representative images of Sirius red staining under polarization microscopy. Scale bar, 50 μm. **Right**, Quantification of collagen quality (defined by OR:YG ratio) in the infarct zone 14 days post-MI among the indicated groups. n=5 to 10 per group. **F**, Summary data for the collagen fibril diameter analysis of electron microscopic images from the infarct scars among the indicated groups. n=3 per group. **G**, Cardiac fibroblasts were separately cultured or cocultured with control lentivirus-treated Tregs or Sparc-overexpressing lentivirus-treated Tregs for 24 hours. RT-PCR analysis of *Col1a1*, *Col3a1*, and *ASMA* mRNA expression of the cardiac fibroblasts in the indicated groups. n=5 per group. Statistical comparisons: 2-way ANOVA with Tukey post hoc test or nonparametric Scheirer-Ray-Hare test were performed in **A** through **E**; 1-way ANOVA with the Tukey multiple comparison test was performed in **G**. **P*<0.05, ***P*<0.01. Ad-Ctrl indicates control adenovirus; Ad-Sparc, secreted acidic cysteine-rich glycoprotein–overexpressing adenoviral vector; ASMA, α-smooth muscle actin; A.U., arbitrary unit; CD, cluster of differentiation; CFs, cardiac fibroblasts; DAPI, 4′,6-diamidino-2-phenylindole; IgG, immunoglobulin G; Lenti-Ctrl, control lentivirus; Lenti-Sparc, secreted acidic cysteine-rich glycoprotein–overexpressing lentivirus; OR, orange-red; YG, yellow-green; RT-PCR, reverse transcription polymerase chain reaction; and Tregs, regulatory T cells.

heart Tregs through both gain- and lose-of-function experiments, which was consistent with our recent report on abdominal aortic aneurysm.[35] Regarding the mechanism of IL-33–induced Treg expansion, we showed that IL-33 injection enhanced the proliferation of Tregs. Another possible mechanism is whether IL-33 promoted heart Treg recruitment from circulation. In injured skeletal muscle, Kuswanto et al[16] ruled out this possibility. Because most heart Tregs (≈90%) were in cell cycle, we considered that amplification rather than recruitment was the major contributor to IL-33/ST2 action on heart Tregs. Previous studies have demonstrated that IL-33 attenuates cardiac remodeling after MI,[36,37] which is consistent with a protective role of Tregs. Here, we showed that IL-33 significantly expanded heart Tregs, which represented a possible mechanism underlying the protection of IL-33 on MI.

Heart Tregs Promote Scar Repair, With Sparc as a Functional Mediator

The transcriptomic data showed an upregulation of extracellular matrix proteins and collagen-related genes of heart Tregs, indicating enhanced ability to promote the repair after MI. Thus, considering the traits of tissue Tregs, heart Tregs are more likely to play a cardioprotective role by directly promoting repair in relation to suppressing inflammation. Among these differentially expressed transcripts, *Sparc* is a prime example that has little expression in the lymphoid Tregs but is highly expressed by heart Tregs. Its corresponding product Sparc is an important cellular matrix protein that mediates cell-matrix interactions and regulates the production and assembly of extracellular matrices.[38] In mice, the absence of Sparc increases the rate of mortality attributable to heart rupture and dysfunction after MI.[28] This effect is mainly caused by impaired granulation tissue formation and collagen maturation after *Sparc* knockout.[28] Our data demonstrated that Sparc overexpression decreased mortality and cardiac rupture in Treg-ablated mice, which was associated with increased collagen content and enhanced maturation in the infarct scars, making up for the defects in tissue repair caused by Treg removal. However, except for Tregs, other Sparc-producing cells (including fibroblasts and macrophages) may also contribute to the effect of Sparc in MI settings. Thus, we further overexpressed Sparc on Tregs in vitro, and their effect on collagen was consistent with that in vivo. To directly address that Treg-derived Sparc is responsible for driving collagen synthesis and maturation in vivo, mice that specifically knock out Sparc in Tregs would be needed. In addition to Sparc, heart Tregs also highly expressed Areg, a functional mediator of Tregs in skeletal muscle[6] and lung tissue,[39] and a group of extracellular matrix–related molecules, as well, which indicates that heart Tregs may function through multiple mediators. Whether these molecules also functionally contribute to heart Tregs remains to be determined.

Conclusions and Perspectives

In conclusion, we identified a unique population of heart Tregs with a prorepair phenotype that is mainly migrated from the circulation, coupled with local expansion and phenotypic conversion from Tconvs. Their accumulation is dependent on the IL-33/ST2 axis. These heart Tregs show strong expression of Sparc and play a necessary protective role in preserving cardiac integrity after MI by increasing collagen content and promoting maturation in the infarct scars. Harnessing the power of heart Tregs may therefore lead to the development of new treatment strategies for MI and other cardiac diseases.

ARTICLE INFORMATION

Received March 14, 2020; accepted September 2, 2020.

The Data Supplement is available with this article at https://www.ahajournals.org/doi/suppl/10.1161/CIRCULATIONAHA.120.046789.

Correspondence

Xiang Cheng, MD, PhD, Department of Cardiology, Union Hospital, Tongji Medical College, Huazhong University of Science and Technology, and Key Laboratory of Biological Targeted Therapy of the Ministry of Education, 1277 Jiefang Rd, Jianghan District, Wuhan 430000, Hubei, China. Email nathancx@hust.edu.cn

Affiliations

Department of Cardiology, Union Hospital, and Key Laboratory of Biological Targeted Therapy of the Ministry of Education (N.X., Y. Lu, M.G., N.L., M.L., J.J., Z.Z., J.L., D.L., T.T., B.L., S.N., M.Z., M.L., Y. Liao, X.C.), Department of Immunology (X.Y.), Tongji Medical College, Huazhong University of Science and Technology, Wuhan, China.

Acknowledgments

We thank Prof McKenzie (Medical Research Council Laboratory of Molecular Biology, University of Cambridge, Cambridge, United Kingdom) for providing the *Il1rl1*$^{-/-}$ mice. We also thank J. Min (Wuhan Institute of Virology, Chinese Academy of Sciences) for kindly assisting us with fluorescence-activated cell sorting.

Sources of Funding

This work was supported by grants from the National Natural Science Foundation of China (No. 81525003, 81720108005, 91639301, and 82030016 to Dr Cheng; No. 81770503 and 81400364 to Dr Xia; No. 81900451 to Dr Lu; No. 81670361 and 81974037 to Dr Tang; No. 81600287 to Dr Zhu; No. 81600390 to Dr Liao), and the 2017 Chang Jiang Scholars Program (T2017073 to Dr Cheng).

Disclosures

None.

Supplemental Materials

Data Supplement Methods
Data Supplement Tables I–III
Data Supplement Figures I–VIII
References 40–59

REFERENCES

1. Sakaguchi S, Ono M, Setoguchi R, Yagi H, Hori S, Fehervari Z, Shimizu J, Takahashi T, Nomura T. Foxp3+ CD25+ CD4+ natural regulatory T cells in dominant self-tolerance and autoimmune disease. *Immunol Rev.* 2006;212:8–27. doi: 10.1111/j.0105-2896.2006.00427.x
2. Josefowicz SZ, Lu LF, Rudensky AY. Regulatory T cells: mechanisms of differentiation and function. *Annu Rev Immunol.* 2012;30:531–564. doi: 10.1146/annurev.immunol.25.022106.141623
3. Panduro M, Benoist C, Mathis D. Tissue Tregs. *Annu Rev Immunol.* 2016;34:609–633. doi: 10.1146/annurev-immunol-032712-095948
4. Cipolletta D, Feuerer M, Li A, Kamei N, Lee J, Shoelson SE, Benoist C, Mathis D. PPAR-γ is a major driver of the accumulation and phenotype of adipose tissue Treg cells. *Nature.* 2012;486:549–553. doi: 10.1038/nature11132
5. Feuerer M, Herrero L, Cipolletta D, Naaz A, Wong J, Nayer A, Lee J, Goldfine AB, Benoist C, Shoelson S, et al. Lean, but not obese, fat is enriched for a unique population of regulatory T cells that affect metabolic parameters. *Nat Med.* 2009;15:930–939. doi: 10.1038/nm.2002
6. Burzyn D, Kuswanto W, Kolodin D, Shadrach JL, Cerletti M, Jang Y, Sefik E, Tan TG, Wagers AJ, Benoist C, Mathis D. A special population of regulatory T cells potentiates muscle repair. *Cell.* 2013;155:1282–1295. doi: 10.1016/j.cell.2013.10.054
7. Tan TG, Mathis D, Benoist C. Singular role for T-BET+CXCR3+ regulatory T cells in protection from autoimmune diabetes. *Proc Natl Acad Sci U S A.* 2016;113:14103–14108. doi: 10.1073/pnas.1616710113
8. Ali N, Zirak B, Rodriguez RS, Pauli ML, Truong HA, Lai K, Ahn R, Corbin K, Lowe MM, Scharschmidt TC, et al. Regulatory T cells in skin facilitate epithelial stem cell differentiation. *Cell.* 2017;169:1119–1129.e11.
9. Ito M, Komai K, Mise-Omata S, Iizuka-Koga M, Noguchi Y, Kondo T, Sakai R, Matsuo K, Nakayama T, Yoshie O, et al. Brain regulatory T cells suppress astrogliosis and potentiate neurological recovery. *Nature.* 2019;565:246–250. doi: 10.1038/s41586-018-0824-5
10. Mock JR, Dial CF, Tune MK, Norton DL, Martin JR, Gomez JC, Hagan RS, Dang H, Doerschuk CM. Transcriptional analysis of Foxp3+ Tregs and functions of two identified molecules during resolution of ALI. *JCI Insight.* 2019;4:e124958.
11. Clarke SA, Richardson WJ, Holmes JW. Modifying the mechanics of healing infarcts: is better the enemy of good? *J Mol Cell Cardiol.* 2016;93:115–124.
12. Weirather J, Hofmann UD, Beyersdorf N, Ramos GC, Vogel B, Frey A, Ertl G, Kerkau T, Frantz S. Foxp3$^+$ CD4$^+$ T cells improve healing after myocardial infarction by modulating monocyte/macrophage differentiation. *Circ Res.* 2014;115:55–67. doi: 10.1161/CIRCRESAHA.115.303895
13. Sharir R, Semo J, Shimoni S, Ben-Mordechai T, Landa-Rouben N, Maysel-Auslender S, Shaish A, Entin-Meer M, Keren G, George J. Experimental myocardial infarction induces altered regulatory T cell hemostasis, and adoptive transfer attenuates subsequent remodeling. *PLoS One.* 2014;9:e113653.
14. Tang T, Yuan J, Zhu Z, Zhang W, Xiao H, Xia N, Yan X, Nie S, Liu J, Zhou S, et al. Regulatory T cells ameliorate cardiac remodeling after myocardial infarction. *Basic Res Cardiol.* 2012;107:232.
15. Hill JA, Feuerer M, Tash K, Haxhinasto S, Perez J, Melamed R, Mathis D, Benoist C. Foxp3 transcription-factor-dependent and -independent regulation of the regulatory T cell transcriptional signature. *Immunity.* 2007;27:786–800.
16. Kuswanto W, Burzyn D, Panduro M, Wang KK, Jang YC, Wagers AJ, Benoist C, Mathis D. Poor repair of skeletal muscle in aging mice reflects a defect in local, interleukin-33-dependent accumulation of regulatory T cells. *Immunity.* 2016;44:355–367.
17. Kunkel GT, Maceyka M, Milstien S, Spiegel S. Targeting the sphingosine-1-phosphate axis in cancer, inflammation and beyond. *Nat Rev Drug Discov.* 2013;12:688–702. doi: 10.1038/nrd4099
18. Sager HB, Hulsmans M, Lavine KJ, Moreira MB, Heidt T, Courties G, Sun Y, Iwamoto Y, Tricot B, Khan OF, et al. Proliferation and recruitment contribute to myocardial macrophage expansion in chronic heart failure. *Circ Res.* 2016;119:853–864.
19. Butler A, Hoffman P, Smibert P, Papalexi E, Satija R. Integrating single-cell transcriptomic data across different conditions, technologies, and species. *Nat Biotechnol.* 2018;36:411–420.
20. Zhang L, Yu X, Zheng L, Zhang Y, Li Y, Fang Q, Gao R, Kang B, Zhang Q, Huang JY, et al. Lineage tracking reveals dynamic relationships of T cells in colorectal cancer. *Nature.* 2018;564:268–272.
21. Amir el AD, Davis KL, Tadmor MD, Simonds EF, Levine JH, Bendall SC, Shenfeld DK, Krishnaswamy S, Nolan GP, Pe'er D. viSNE enables visualization of high dimensional single-cell data and reveals phenotypic heterogeneity of leukemia. *Nat Biotechnol.* 2013;31:545–552.
22. Shevach EM, Thornton AM. tTregs, pTregs, and iTregs: similarities and differences. *Immunol Rev.* 2014;259:88–102. doi: 10.1111/imr.12160
23. Bilate AM, Lafaille JJ. Induced CD4$^+$Foxp3$^+$ regulatory T cells in immune tolerance. *Annu Rev Immunol.* 2012;30:733–758.
24. Thornton AM, Korty PE, Tran DQ, Wohlfert EA, Murray PE, Belkaid Y, Shevach EM. Expression of Helios, an Ikaros transcription factor family member, differentiates thymic-derived from peripherally induced Foxp3$^+$ T regulatory cells. *J Immunol.* 2010;184:3433–3441. doi: 10.4049/jimmunol.0904028
25. Burzyn D, Benoist C, Mathis D. Regulatory T cells in nonlymphoid tissues. *Nat Immunol.* 2013;14:1007–1013.
26. Kolodin D, van Panhuys N, Li C, Magnuson AM, Cipolletta D, Miller CM, Wagers A, Germain RN, Benoist C, Mathis D. Antigen- and cytokine-driven accumulation of regulatory T cells in visceral adipose tissue of lean mice. *Cell Metab.* 2015;21:543–557.
27. Sanada S, Hakuno D, Higgins LJ, Schreiter ER, McKenzie AN, Lee RT. IL-33 and ST2 comprise a critical biomechanically induced and cardioprotective signaling system. *J Clin Invest.* 2007;117:1538–1549.
28. Schellings MW, Vanhoutte D, Swinnen M, Cleutjens JP, Debets J, van Leeuwen RE, d'Hooge J, Van de Werf F, Carmeliet P, Pinto YM, et al. Absence of SPARC results in increased cardiac rupture and dysfunction after acute myocardial infarction. *J Exp Med.* 2009;206:113–123. doi: 10.1084/jem.20081244
29. Richardson WJ, Clarke SA, Quinn TA, Holmes JW. Physiological implications of myocardial scar structure. *Compr Physiol.* 2015;5:1877–1909.
30. Ma Y, de Castro Bras LE, Toba H, Iyer RP, Hall ME, Winniford MD, Lange RA, Tyagi SC, Lindsey ML. Myofibroblasts and the extracellular matrix network in post-myocardial infarction cardiac remodeling. *Pflugers Arch.* 2014;466:1113–1127.
31. Fu X, Khalil H, Kanisicak O, Boyer JG, Vagnozzi RJ, Maliken BD, Sargent MA, Prasad V, Valiente-Alandi I, Blaxall BC, et al. Specialized fibroblast differentiated states underlie scar formation in the infarcted mouse heart. *J Clin Invest.* 2018;128:2127–2143.
32. Rieckmann M, Delgobo M, Gaal C, Buchner L, Steinau P, Reshef D, Gil-Cruz C, Horst ENT, Kircher M, Reiter T, et al. Myocardial infarction triggers cardioprotective antigen-specific T helper cell responses. *J Clin Invest.* 2019;130:4922–4936.
33. Delacher M, Imbusch CD, Hotz-Wagenblatt A, Mallm JP, Bauer K, Simon M, Riegel D, Rendeiro AF, Bittner S, Sanderink L, et al. Precursors for nonlymphoid-tissue Treg cells reside in secondary lymphoid organs and are programmed by the transcription factor BATF. *Immunity.* 2020;52:295–312.e11.
34. Saxena A, Dobaczewski M, Rai V, Haque Z, Chen W, Li N, Frangogiannis NG. Regulatory T cells are recruited in the infarcted mouse myocardium and may modulate fibroblast phenotype and function. *Am J Physiol Heart Circ Physiol.* 2014;307:H1233–H1242.
35. Li J, Xia N, Wen S, Li D, Lu Y, Gu M, Tang T, Jiao J, Lv B, Nie S, Liao M, et al. IL (Interleukin)-33 suppresses abdominal aortic aneurysm by enhancing regulatory T-cell expansion and activity. *Arterioscler Thromb Vasc Biol.* 2019;39:446–458. doi: 10.1161/ATVBAHA.118.312023
36. Yin H, Li P, Hu F, Wang Y, Chai X, Zhang Y. IL-33 attenuates cardiac remodeling following myocardial infarction via inhibition of the p38

MAPK and NF-κB pathways. *Mol Med Rep.* 2014;9:1834–1838. doi: 10.3892/mmr.2014.2051
37. Li J, Shen D, Tang J, Wang Y, Wang B, Xiao Y, Cao C, Shi X, Liu HM, Zhao W, et al. IL33 attenuates ventricular remodeling after myocardial infarction through inducing alternatively activated macrophages ethical standards statement. *Eur J Pharmacol.* 2019;854:307–319. doi: 10.1016/j.ejphar.2019.04.046
38. Dobaczewski M, Gonzalez-Quesada C, Frangogiannis NG. The extracellular matrix as a modulator of the inflammatory and reparative response following myocardial infarction. *J Mol Cell Cardiol.* 2010;48:504–511. doi: 10.1016/j.yjmcc.2009.07.015
39. Arpaia N, Green JA, Moltedo B, Arvey A, Hemmers S, Yuan S, Treuting PM, Rudensky AY. A distinct function of regulatory T cells in tissue protection. *Cell.* 2015;162:1078–1089.
40. Tang TT, Li YY, Li JJ, Wang K, Han Y, Dong WY, Zhu ZF, Xia N, Nie SF, Zhang M, et al. Liver-heart crosstalk controls IL-22 activity in cardiac protection after myocardial infarction. *Theranostics.* 2018;8:4552–4562. doi: 10.7150/thno.24723
41. Xia N, Jiao J, Tang TT, Lv BJ, Lu YZ, Wang KJ, Zhu ZF, Mao XB, Nie SF, Wang Q, et al. Activated regulatory T-cells attenuate myocardial ischaemia/reperfusion injury through a CD39-dependent mechanism. *Clin Sci (Lond).* 2015;128:679–693. doi: 10.1042/CS20140672
42. Paik DT, Rai M, Ryzhov S, Sanders LN, Aisagbonhi O, Funke MJ, Feoktistov I, Hatzopoulos AK. Wnt10b gain-of-function improves cardiac repair by arteriole formation and attenuation of fibrosis. *Circ Res.* 2015;117:804–816. doi: 10.1161/CIRCRESAHA.115.306886
43. van den Bos EJ, Mees BM, de Waard MC, de Crom R, Duncker DJ. A novel model of cryoinjury-induced myocardial infarction in the mouse: a comparison with coronary artery ligation. *Am J Physiol Heart Circ Physiol.* 2005;289:H1291–H1300.
44. Benakis C, Brea D, Caballero S, Faraco G, Moore J, Murphy M, Sita G, Racchumi G, Ling L, Pamer EG, et al. Commensal microbiota affects ischemic stroke outcome by regulating intestinal gammadelta T cells. *Nat Med.* 2016;22:516–523.
45. Wagers AJ, Sherwood RI, Christensen JL, Weissman IL. Little evidence for developmental plasticity of adult hematopoietic stem cells. *Science.* 2002;297:2256–2259. doi: 10.1126/science.1074807
46. Barker TH, Baneyx G, Cardó-Vila M, Workman GA, Weaver M, Menon PM, Dedhar S, Rempel SA, Arap W, Pasqualini R, et al. SPARC regulates extracellular matrix organization through its modulation of integrin-linked kinase activity. *J Biol Chem.* 2005;280:36483–36493. doi: 10.1074/jbc.M504663200
47. He TC, Zhou S, da Costa LT, Yu J, Kinzler KW, Vogelstein B. A simplified system for generating recombinant adenoviruses. *Proc Natl Acad Sci U S A.* 1998;95:2509–2514. doi: 10.1073/pnas.95.5.2509
48. Mortazavi A, Williams BA, McCue K, Schaeffer L, Wold B. Mapping and quantifying mammalian transcriptomes by RNA-Seq. *Nat Methods.* 2008;5:621–628. doi: 10.1038/nmeth.1226
49. Garber M, Grabherr MG, Guttman M, Trapnell C. Computational methods for transcriptome annotation and quantification using RNA-seq. *Nat Methods.* 2011;8:469–477. doi: 10.1038/nmeth.1613
50. Anders S, Huber W. Differential expression analysis for sequence count data. *Genome Biol.* 2010;11:R106.
51. Love MI, Huber W, Anders S. Moderated estimation of fold change and dispersion for RNA-seq data with DESeq2. *Genome Biol.* 2014;15:550. doi: 10.1186/s13059-014-0550-8
52. Villalobos E, Criollo A, Schiattarella GG, Altamirano F, French KM, May HI, Jiang N, Nguyen NUN, Romero D, Roa JC, et al. Fibroblast primary cilia are required for cardiac fibrosis. *Circulation.* 2019;139:2342–2357. doi: 10.1161/CIRCULATIONAHA.117.028752
53. Yan X, Zhang H, Fan Q, Hu J, Tao R, Chen Q, Iwakura Y, Shen W, Lu L, Zhang Q, et al. Dectin-2 deficiency modulates Th1 differentiation and improves wound healing after myocardial infarction. *Circ Res.* 2017;120:1116–1129. doi: 10.1161/CIRCRESAHA.116.310260
54. Lee SJ, Lee CK, Kang S, Park I, Kim YH, Kim SK, Hong SP, Bae H, He Y, Kubota Y, et al. Angiopoietin-2 exacerbates cardiac hypoxia and inflammation after myocardial infarction. *J Clin Invest.* 2018;128:5018–5033. doi: 10.1172/JCI99659
55. Liu L, Jin X, Hu CF, Zhang YP, Zhou Z, Li R, Shen CX. Amphiregulin enhances cardiac fibrosis and aggravates cardiac dysfunction in mice with experimental myocardial infarction partly through activating EGFR-dependent pathway. *Basic Res Cardiol.* 2018;113:12. doi: 10.1007/s00395-018-0669-y
56. Van Aelst LN, Voss S, Carai P, Van Leeuwen R, Vanhoutte D, Sanders-van Wijk S, Eurlings L, Swinnen M, Verheyen FK, Verbeken E, et al. Osteoglycin prevents cardiac dilatation and dysfunction after myocardial infarction through infarct collagen strengthening. *Circ Res.* 2015;116:425–436. doi: 10.1161/CIRCRESAHA.116.304599
57. Kong P, Shinde AV, Su Y, Russo I, Chen B, Saxena A, Conway SJ, Graff JM, Frangogiannis NG. Opposing actions of fibroblast and cardiomyocyte Smad3 signaling in the infarcted myocardium. *Circulation.* 2018;137:707–724. doi: 10.1161/CIRCULATIONAHA.117.029622
58. Westermann D, Mersmann J, Melchior A, Freudenberger T, Petrik C, Schaefer L, Lullmann-Rauch R, Lettau O, Jacoby C, Schrader J, et al. Biglycan is required for adaptive remodeling after myocardial infarction. *Circulation.* 2008;117:1269–1276.
59. Pinto AR, Ilinykh A, Ivey MJ, Kuwabara JT, D'Antoni ML, Debuque R, Chandran A, Wang L, Arora K, Rosenthal NA, et al. Revisiting cardiac cellular composition. *Circ Res.* 2016;118:400–409. doi: 10.1161/CIRCRESAHA.115.307778